Dairy biogas as fuel for a Molten Carbonate Fuel Cell—initial study

Jarosław Milewski[*,a], Karina Michalska[b], Anna Kacprzak[c]

[a]Warsaw University of Technology, Institute of Heat Engineering
21/25 Nowowiejska Street, 00-665 Warsaw, Poland
[b]Textile Research Institute
5/15 Brzezinska Street, 92-103 Lodz, Poland
[c]Technical University of Lodz, Faculty of Process and Environmental Engineering
213 Wolczanska Street, 90-924 Lodz, Poland

Abstract

Based on 0-D mathematical modeling and numerical simulations, the performance a Molten Carbonate Fuel Cell (MCFC) run on dairy biogas is presented.

The governing equations of the MCFC model are presented, the equations were utilized for an adequate simulator construction. An analysis of dairy biogas as fuels for MCFC is presented. The results are compared with hydrogen as a reference fuel. The dairy biogas is characterized by both lower efficiency and lower fuel utilization factors compared to natural gas.

Keywords: biogases, molten carbonate fuel cell, mathematical model

1. Introduction

Fuel price inflation and a long-term increase in electricity consumption have provided added impetus to the search for ultra-effective power generation systems. Fuel cells generate power in electrochemical reactions with potentially ultra-high efficiency. High-temperature fuel cells [1] (Solid Oxide Fuel Cell—SOFC [2–6] and Molten Carbonate Fuel Cell—MCFC [7–10]) are considered as highly efficient electricity sources. Presently, state-of-the-art MCFCs are being built in the tens of MW power range. Research and development in this field is predicted to result in an increase in the power of those kinds of systems in the future. Additionally, MCFC can be considered as a very efficient way to separate CO_2 from flue gases [11] competitive to other methods [12, 13] to reduce emissions from fossil fuel power plants [14].

Hydrogen and Natural Gas are currently considered to be the main fuels for fuel cells. Hydrogen is an ideal fuel with respect to fuel cell working conditions. Unfortunately, hydrogen is not present in the environment in an uncombined form and there are difficulties with production, transportation and storage. Natural Gas, meanwhile, is considered to be an interim fuel due to limited resources.

The most plausible future scenarios in the power markets are as follows:

1. Abandoning gas/liquid/solid fuels in favor of electricity generated by renewable sources and/or nuclear plants. In this case, the energy distribution role will be provided by the power grid, and the storage role by consumers.

---

[*]Corresponding author
Email addresses: `milewski@itc.pw.edu.pl` (Jarosław Milewski[*)], `karina.michalska@iw.lodz.pl` (Karina Michalska), `anna.kacprzak@wipos.p.lodz.pl` (Anna Kacprzak)

2. Production of plant-derived gas/liquid fuels based on the cultivation of plants and shrubs, such as e.g. Salix Viminalis and their conversion into fuel, e.g. alcohols [15, 16].

Using electricity only can be problematic (e.g. airplanes), the cultivation of "energy" seems to be one of the most possible scenarios for the future.

The use of biogases in the Molten Carbonate Fuel Cell has been relatively poorly investigated. Landfill-gas (LFG) as a by-product of waste fermentation in landfills was considered as a fuel for the MCFC in [17]. Experimental comparison of MCFC performance using three different biogas types and methane is presented in [18]. The biogases considered are derived from the following processes: steam gasification in an entrained flow gasifier, steam gasification in a duel interconnect fluidized bed gasifier, and biogas from an anaerobic digestion process. In [19] operation of molten carbonate fuel cells with different biogas sources was investigated. Two mobile MCFC test beds were operated with biogas from different origins, and quality and electrical efficiency of the MCFC stack of 50% was achieved. It was also found that there was no severe interaction between biogas and fuel cell system components. In the town of Ahlen (Germany) a molten carbonate fuel cell operated in the municipal sewage system in 2005. It was the first project of its kind in Europe [20]. In [21] an anaerobic digestion process of organic residues was used for electrochemical conversion to electricity and heat through an MCFC. It was shown that during biogas production, H_2S has multiple negative effects on the performance and durability of the MCFC. Three general approaches to solving the sulfur problem in the MCFC are suggested. Much deep analysis about this issue is presented in [22, 23].

Dairy wastes are plentiful in the dairy industries. The wastes contain high levels of organic matter and disposal of the effluents may cause severe environmental pollution [24].

However, sewage and waste from the dairy industry are the ideal raw material for bioenergy production because they contain significant amounts of easily degradable organic pollutants.

In addition, they are characterized by a high content of water and trace elements necessary for the life of microorganisms.

Currently, the ever-increasing energy prices and the growing requirements regarding CO_2 emissions have led to increased interest in alternative energy sources. Biogas plants based on anaerobic processes are an ideal solution for dairy waste utilization while producing energy that can be used universally: for the production of electricity, heat, motor fuel or gas supply.

Anaerobic digestion is attractive because of the increased interest in the recovery of energy from waste. The great interest in the process of anaerobic digestion is caused by its advantages compared to aerobic methods.

Anaerobic decomposition of organic compounds takes place in four phases conducted in close cooperation with various groups of bacteria [25]. These include hydrolyzing, acetogenic, homoacetogenic, sulfate-reducing and methanogenic bacteria [26]. Up to 95% of the organic load in a waste stream can be converted to biogas (methane and carbon dioxide) and the remainder is utilized for cell growth and maintenance.

In the present study, numerical investigation is applied to simulate the behavior of an MCFC run on dairy biogas.

2. Theory

The presented results are based on calculations made using an appropriate mathematical model. The calculations are based on the Lee-Kesler equation of the state and minimization of Gibbs free energy [27].

The maximum voltage of the fuel cell depends on the type of reaction occurring on the electrode surfaces. Biogases in reaction with oxygen can give various maximum voltages. The maximum voltages for various reactions are listed in Table 1.

2.1. Molten Carbonate Fuel Cell

The governing equations of the MCFC model are presented in this section [28]. The presented analysis considers a design point estimation of the MCFC. Usually, the fuel cell characteristic is defined by a voltage-current density curve ($E = f(i)$) but in the case of design point calculations the voltage-fuel utilization factor curve ($E = f(\eta_f)$) becomes the ba-

Table 1: Maximum voltages for various reactions

Component	Chemical Reaction	Maximum Voltage, E_{max}, V
H_2	$H_2 + 1/2O_2 \rightarrow H_2O$	1.23
CH_4	$CH_4 + 2O_2 \rightarrow CO_2 + H_2O$	1.06
CH_3OH	$CH_3OH + 3/2O_2 \rightarrow CO_2 + 2H_2O$	1.22
C	$C + O_2 \rightarrow CO_2$	1.03
C	$C + 1/2O_2 \rightarrow CO$	0.72
CO	$CO + 1/2O_2 \rightarrow CO_2$	1.34

sic characteristic. The other model assumptions are listed below:

1. anode inlet pressure = 1 bar;
2. cathode inlet pressure = 1 bar;
3. temperature = 650°C.

The mixture of various hydrocarbons enters into the MCFC anode, so the fuel utilization factor is calculated based on an equivalent hydrogen molar flow. The equivalent hydrogen molar flow at the anode inlet is defined by the following relationship:

$$\dot{n}_{H_2,equivalent} = \dot{n}_{H_2} + \dot{n}_{CO} + 4 \cdot \dot{n}_{CH_4} \quad (1)$$

From Table 1 it can be seen that biogases in reaction with oxygen can give various maximum voltages. Mixtures of various components occur in the case of the analyzed fuels. Due to these circumstances the general form of Nernst's equation is used to estimate the voltage of MCFC (Eq. 2)). Adequate partial pressures were calculated tusing software [27].

$$E_{\max,MCFC} = \frac{R \cdot T}{4 \cdot F} \ln \frac{p_{O_2,cathode} \cdot p_{CO_2,cathode}^2}{p_{O_2,anode} \cdot p_{CO_2,anode}^2} \quad (2)$$

where: T—absolute temperature; R—universal gas constant; F—Faraday's constant; p—partial pressure.

Eq. 2 is a general form of the Nernst equation and for the hydrogen-oxygen reaction it can be simplified to the following form:

$$K = \frac{p_{H_2O,anode} \cdot p_{ref}}{p_{H_2,anode} \cdot p_{O_2,anode}^{\frac{1}{2}}} = A \cdot e^{-\frac{E_{act}}{R \cdot T}} \quad (3)$$

$$p_{O_2,anode} = \frac{p_{H_2O,anode}^2 \cdot p_{ref}^2}{p_{H_2,anode}^2 \cdot K^2} \quad (4)$$

$$E_{\max} = \frac{R \cdot T}{2 \cdot F} \ln K$$
$$+ \frac{R \cdot T}{2 \cdot F} \ln \frac{p_{H_2,anode} \cdot p_{O_2,cathode}^{\frac{1}{2}}}{p_{H_2O,anode}} \quad (5)$$
$$+ \frac{R \cdot T}{2 \cdot F} \ln \frac{p_{CO_2,cathode}}{p_{CO_2,anode}}$$

where: K—chemical equilibrium constant, p_{ref}—reference pressure (often assumed to be 1).

Two types of resistance are present in fuel cells: ionic resistance r_1 and electric resistance r_2. Thus, voltage generated by a single cell is given by the following equation:

$$E_{MCFC} = \frac{E_{\max,MCFC} - \eta \cdot i_{\max} \cdot r_1}{\frac{r_1}{r_2} \cdot \left(1 - \eta_f\right) + 1} \quad (6)$$

where: η—utilization factor; $i_{\max}$—maximum current density; r_1—internal ionic area specific resistance of the cell; r_2—internal electronic area specific resistance of the cell.

The internal area specific ionic resistance can be described by the following relationship:

$$r_1 = \frac{\delta}{\sigma} \quad (7)$$

where: δ—electrolyte matrix thickness; σ—ionic conductivity of molten carbonate.

The ionic conductivity of the carbonate is defined as follows:

$$\sigma = \sigma_0 \cdot e^{\frac{-E_{act}}{R \cdot T}} \quad (8)$$
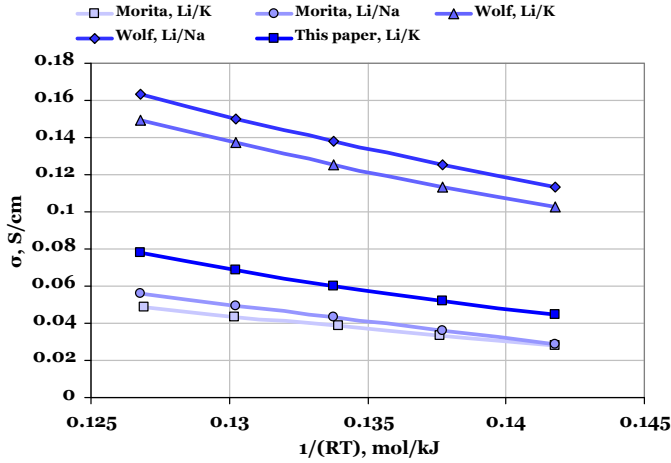
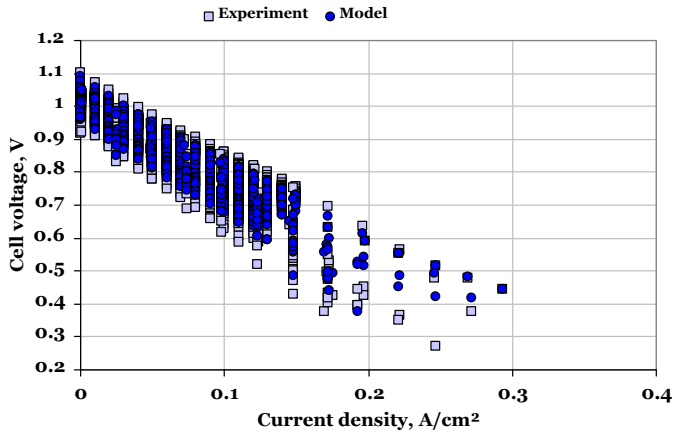Figure 1: Temperature dependence of ionic conductivity for molten carbonates

Figure 2: Experimental and simulations data at different anode and cathode inlet molar fractions, 1,130 experimental points with standard deviation value at level of 2%

where: σ_0, S/cm; E_{act}, kJ/mol—factors dependent on material used.

The ionic resistance of molten carbonate electrolytes as a function of temperature is shown in Fig. 1. This diagram contains values obtained by the researchers' own calculations, which were based on data obtained by their own experiments together with data published by Morita et al. [29] and Wolf et al. [30].

The influences of temperature and electrolyte thickness on electronic internal resistance (r_2) of the electrolytes are not well known. It was assumed that the thickness of the Li/K electrolyte matrix was 0.9 mm, for which the r_2 value is 162 cm^2/S, was determined by the researchers' own calculations, which

Table 3: Characteristics of the individual substrates used in the investigation

Substrate	Total Solids, %	Volatile Solids, %
Clean cheese whey	7.42	6.45
Polluted cheese whey	5.44	4.73
Refused fat	6.38	5.99
Sediment	0.17	0.07
Digested sludge	22.93	16.03

were based on experiments performed. The presented model was compared with experimental data; this comparison is shown in Fig. 2.

3. Experimental

During the investigation the following parameters were determined: Total Solids (TS, drying at a constant temperature of 105°C), Volatile Solids (VS, mineralization in an oven at a constant temperature of 550°C). The biogas content: O_2, N_2, CH_4 and CO_2 was measured by GC analysis (Gas Chromatograph SRI 8610C, SRI Instruments, Inc, USA equipped with TCD Detector; column temperature 60°C, detector temperature 150°C, carrier gas He at a flow rate of 10 mL/min).

The waste samples obtained from a dairy manufacturer located in the Lodz region were mixed with 350 mL of digested sludge obtained from the Group Wastewater Treatment Plant in Lodz, Poland. The waste samples included: clean or polluted cheese whey, refused fat and sediment from the decanter. The description of the samples used in the experimental step is shown in Table 2. The characteristics of the individual substrates is given in Table 3. After mixing, the pH of the mixture was adjusted to 7 using NaHCO$_3$ or H$_2$SO$_4$ and the flasks were placed at 37°C and shaken once per day. Volumes of biogas evolved were measured by the liquid displacement method with the use of 33% NaCl solution. The concentration of methane, carbon dioxide, oxygen and nitrogen content in biogas produced was measured by gas chromatography analysis.

Table 2: Description of the samples used in the investigation

Sample	Description
1	100 mL of clean cheese whey + 1 g of fat + 350 mL of digested sludge
2	100 mL of clean cheese whey + 2 g of fat + 350 mL of digested sludge
3	100 mL of clean cheese whey + 3 g of fat + 350 mL of digested sludge
4	75 mL of clean cheese whey + 1 g of fat + 25 mL of sediment + 350 mL of digested sludge
5	75 mL of clean cheese whey + 2 g of fat + 25 mL of sediment + 350 mL of digested sludge
6	75 mL of clean cheese whey + 3 g of fat + 25 mL of sediment + 350 mL of digested sludge
7	100 mL of polluted cheese whey + 2 g of fat + 350 mL of digested sludge
8	Blank—350 mL of digested sludge

Table 4: Biogas content for each sample used in form simulations with MCFC

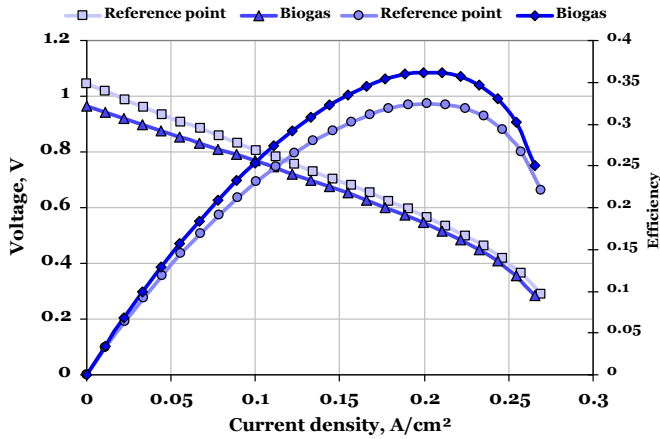| Sample	O_2, %	N_2, %	CH_4, %	CO_2, %	H_2 , %	H_2O, %
1	0.816	3.08	72.2	23.9	–	–
2	0.249	1.35	72.7	25.7	–	–
3	1.04	3.70	69.6	25.6	–	–
4	0.941	3.51	71.0	24.6	–	–
5	3.06	10.4	62.6	24.0	–	–
6	1.15	4.31	69.2	25.3	–	–
7	0.180	0.749	70.6	28.5	–	–
8	0.467	25.7	41.1	32.8	–	–
Reference Point	–	–	–	23	69	8

Figure 3: Current density-voltage curves for the Reference Point and simulated biogas

Biogas with the optimal methane content was used in the investigation into use of the MCFC. It was tapped on the 7th day of the anaerobic digestion process. The biogas content used in the MCFC tests for each sample is shown in Table 4.

4. Results

Presented results are based on both experimental investigations (biogas production) and mathematical modeling (MCFC). The model of MCFC was compared against experimental data obtained for the Reference Point.

MCFC voltages and obtained efficiencies for the analyzed biogas are shown in Fig. 3. The figure contains the cell voltages and efficiencies for the Reference Point and simulated biogas as a function of the current density. The higher open circuit voltage is achieved with hydrogen (Reference Point), but that does not automatically translate into the greatest efficiency for higher current densities. The higher efficiency obtained for methane is explained by internal reforming of methane into hydrogen in the following reactions:

$$CH_4 + H_2O \rightarrow CO + 3H_2 \qquad (9)$$

$$CO + H_2O \rightleftarrows CO_2 + H_2 \qquad (10)$$
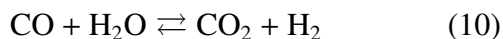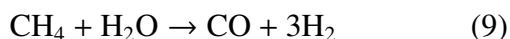
Summing up, both reactions are endothermal, which means that part of the thermal energy released during the reactions is converted back into fuel (hydrogen). In total, the amount of fuel available on the anode side is greater than the fuel flow delivered to the fuel cell.

In terms of energy equivalence, one particle of methane is equivalent to 4 particles of hydrogen (compare reactions 9 and 10).

It should be noted that hydrogen-based reactions are characterized by quite rapid kinetics, at 800°C chemical equilibrium is obtained in 0.04 s. In contrast to hydrogen, methane has quite slow kinetics (e.g. the state of chemical equilibrium is achieved in a few thousand years for the same temperature) [31]. Chemical equilibrium is assumed at the anode, which is mainly true in the case of hydrogen as a fuel. For other fuels, adequate kinetic calculations must be made to obtain an accurate value of oxygen partial pressure [32]. Additionally, the presence of a catalytic medium [33] can impact the manner of obtaining accurate results.

5. Conclusions

A numerical simulation was used to estimate the working conditions of a laboratory size fuel cell working on biogas produced from dairy waste. An adequate mathematical model of the MCFC was built and is commented on in the paper.

Two fuels were taken into consideration (hydrogen and a biogas-steam mixture). For both fuels, the calculations for the chemical reactions were based on minimizing free Gibbs energy (the chemical equilibrium state) which might be far removed from the real conditions for methane, but should be very close to reality for hydrogen.

For both fuels, moderate efficiencies were obtained (30% for hydrogen and 35% for biogas).

In the near future, the obtained results will be validated through the use of a real experimental labstand.

References

[1] D. Bakalis, A. Stamatis, Incorporating available micro gas turbines and fuel cell: Matching considerations and performance evaluation, Applied Energy 103 (2013) 607–617.

[2] P. Pianko-Oprych, Z. Jaworski, Numerical modelling of the micro-tubular solid oxide fuel cell stacks [przeglad metod modelowania numerycznego mikrorurowych stał otlenkowych stosów ognhw paliwowych], Przemysl Chemiczny 91 (9) (2012) 1813–1815.

[3] H. Marzooghi, M. Raoofat, M. Dehghani, G. Elahi, Dynamic modeling of solid oxide fuel cell stack based on local linear model tree algorithm, International Journal of Hydrogen Energy 37 (5) (2012) 4367–4376.

[4] K. Chaichana, Y. Patcharavorachot, B. Chutichai, D. Saebea, S. Assabumrungrat, A. Arpornwichanop, Neural network hybrid model of a direct internal reforming solid oxide fuel cell, International Journal of Hydrogen Energy 37 (3) (2012) 2498–2508.

[5] S. Bozorgmehri, M. Hamedi, Modeling and optimization of anode-supported solid oxide fuel cells on cell parameters via artificial neural network and genetic algorithm, Fuel Cells 12 (1) (2012) 11–23.

[6] J. Qian, Z. Tao, J. Xiao, G. Jiang, W. Liu, Performance improvement of ceria-based solid oxide fuel cells with yttria-stabilized zirconia as an electronic blocking layer by pulsed laser deposition, International Journal of Hydrogen Energy 38 (5) (2013) 2407–2412.

[7] D. Sanchez, R. Chacartegui, J. M. de Escalona, A. Munoz, T. Sanchez, Performance analysis of a MCFC & supercritical carbon dioxide hybrid cycle under part load operation, International Journal of Hydrogen Energy 36 (16) (2011) 10327 – 10336.

[8] H. Jeong, S. Cho, D. Kim, H. Pyun, D. Ha, C. Han, M. Kang, M. Jeong, S. Lee, A heuristic method of variable selection based on principal component analysis and factor analysis for monitoring in a 300 kw mcfc power plant, International Journal of Hydrogen Energy 37 (15) (2012) 11394–11400.

[9] G. De Lorenzo, P. Fragiacomo, Electrical and electrical-thermal power plants with molten carbonate fuel cell/gas turbine-integrated systems, International Journal of Energy Research 36 (2) (2012) 153–165.

[10] C.-G. Lee, D.-H. Kim, H.-C. Lim, Electrode reaction characteristics under pressurized conditions in a molten carbonate fuel cell, Journal of the Electrochemical Society 154 (4) (2007) B396–B404.

[11] G. Discepoli, G. Cinti, U. Desideri, D. Penchini, S. Proietti, Carbon capture with molten carbonate fuel cells: Experimental tests and fuel cell performance assessment, International Journal of Greenhouse Gas Control 9 (2012) 372–384.

[12] L. Bartela, A. Skorek-Osikowska, J. Kotowicz, Integration of a supercritical coal-fired heat and power plant with carbon capture installation and gas turbine [integracja bloku elektrociepłowni weglowej na parametry nadkrytyczne z instalacja wychwytu dwutlenku wegla oraz turbina gazowa], Rynek Energii 100 (3) (2012) 56–62.

[13] K. Janusz-Szymańska, Economic efficiency of an igcc system integreted with ccs installation [efektywność ekonomiczna układu gazowo-parowego zintegrowanego ze zgazowaniem węgla oraz z instalacjaą CCS], Rynek Energii 102 (5) (2012) 24–30.

[14] W. Bujalski, Optimization of electricity and heat generation in large chp plant equipped with a heat accumulator, Rynek Energii 101 (4) (2012) 131–136.

[15] A. Sobolewski, . Bartela, A. Skorek-Osikowska, T. Iluk, Comparison of the economic efficiency of chp plants integrated with gazela generator [porównanie efektywności ekonomicznej układów kogeneracyjnych z generatorem gazu procesowego gazela], Rynek Energii 102 (5) (2012) 31–37.

[16] J. Kupecki, J. Jewulski, K. Badyda, Comparative study of biogas and dme fed micro-chp system with solid oxide fuel cell, Applied Mechanics and Materials 267 (2013) 53–56.

[17] P. Lunghi, R. Bove, U. Desideri, Life-cycle-assessment of fuel-cells-based landfill-gas energy conversion technologies, Journal of Power Sources 131 (1–2) (2004) 120 – 126.

[18] R. Bove, P. Lunghi, Experimental comparison of mcfc performance using three different biogas types and methane, Journal of Power Sources 145 (2005) 588–593.

[19] S. Trogisch, J. Hoffmann, L. Bertrand, Operation of molten carbonate fuel cells with different biogas sources: A challenging approach for field trials, Journal of Power Sources 145 (2005) 632–638.

[20] M. Krumbeck, T. Klinge, B. Doging, First european fuel cell installation with anaerobic digester gas in a molten carbonate fuel cell, Journal of Power Sources 157 (2006) 902–905.

[21] R. Ciccoli, V. Cigolotti, R. L. Presti, E. Massi, S. McPhail, G. Monteleone, A. Moreno, V. Naticchioni, C. Paoletti, E. Simonetti, F. Zaza, Molten carbonate fuel cells fed with biogas: Combating h2s, Waste Management 30 (6) (2010) 1018 – 1024.

[22] F. Zaza, C. Paoletti, R. LoPresti, E. Simonetti, M. Pasquali, Studies on sulfur poisoning and development of advanced anodic materials for waste-to-energy fuel cells applications, Journal of Power Sources 195 (13) (2010) 4043 – 4050.

[23] F. Zaza, C. Paoletti, R. LoPresti, E. Simonetti, M. Pasquali, Multiple regression analysis of hydrogen sulphide poisoning in molten carbonate fuel cells used for waste-to-energy conversions, International Journal of Hydrogen Energy 36 (13) (2011) 8119 – 8125.

[24] S. Patil, N. Ghasghse, A. Nashte, S. Kanase, R. Powar, Anaerobic digestion treatment of cheese whey for production of methane in a two stage upflow packed bed reactor, International Journal of Advanced Science 1 (2012) 1–7.

[25] G. Lastella, C. Testa, G. Cornacchia, M. Notornicola, F. Voltasio, V. K. Sharma, Anaerobic digestion of semi-solid organic waste: Biogas production and its purification, Energy Conservation & Management 43 (2002) 63–75.

[26] D. Chynoweth, J. Owens, R. Legrand, Renewable methane from anaerobic digestion of biomass, Renewable Energy 22 (2001) 1–8.

[27] Hyprotech Corporation, HYSYS.Plant Steady State Modelling (1998).

[28] J. Milewski, M. Wołowicz, A. Miller, An alternative model of molten carbonate fuel cell: A proposal, in: EmHyTeC 2012, no. P.1-34, 2012, pp. 130–132.

[29] H. Morita, M. Komoda, Y. Mugikura, Y. Izaki, T. Watanabe, Y. Masuda, T. Matsuyama, Performance analysis of molten carbonate fuel cell using a li/na electrolyte, Journal of Power Sources 112 (2) (2002) 509 – 518.

[30] T. Wolf, G. Wilemski, Molten carbonate fuel cell performance model, Journal of Electrochemical Society 30 (1983) 48–55.

[31] J. Milewski, K. Świrski, M. Santarelli, P. Leone, Advanced Methods of Solid Oxide Fuel Cell Modeling, 1st Edition, Springer-Verlag London Ltd., 2011.

[32] J. Milewski, J. Lewandowski, Comparative analysis of time constants in solid oxide fuel cell processes – selection of key processes for modeling power systems, Journal of Power Technologies 91 (1) (2011) 1–5.

[33] W. Budzianowski, Role of catalytic technologies in combustion of gaseous fuels, Rynek Energii 82 (3) (2009) 59–63.